HHS Public Access

Author manuscript

Eur Biophys J. Author manuscript; available in PMC 2024 July 01.

Published in final edited form as:

Eur Biophys J. 2023 July ; 52(4-5): 303–310. doi:10.1007/s00249-023-01640-5.

A spectral decomposition quality assessment tool for multi-wavelength AUC experiments with UltraScan

Saeed Mortezazadeh[1], **Borries Demeler**[1,2]

[1]Deptartment of Chemistry and Biochemistry, University of Lethbridge, Lethbridge, AB T1K 3M4, Canada

[2]Deptartment of Chemistry and Biochemistry, University of Montana, Missoula, MT 59812, USA

Abstract

Multi-wavelength analytical ultracentrifugation (MW-AUC) is a recently developed technique that has proven to be a promising tool to investigate mixtures of molecules containing multiple chromophores. It provides an orthogonal separation approach by distinguishing molecules based on their spectral and hydrodynamic properties. Existing software implementations do not permit the user to assess the integrity of the spectral decomposition. To address this shortcoming, we developed a new spectral decomposition residual visualization module, which monitors the accuracy of the spectral decomposition. This module assists the user by providing visual and statistical feedback from the decomposition. The software has been integrated into the UltraScan software suite and an example of a mixture containing thyroglobulin and DNA is presented for illustration purposes.

Keywords

Multi-wavelength analytical ultracentrifugation; Spectral decomposition; Statistical metrics; Data fitting; UltraScan

Introduction

Multi-wavelength analytical ultracentrifugation (MW-AUC) is a recent but already well-established technique that relies on collecting AUC data over a range of wavelengths to not only observe the hydrodynamic properties of the molecules present in a mixture, but also separate them based on their spectral properties (Demeler 2019; Henrickson et al. 2022). The first fiber-based UV–visible multi-wavelength detector was originally developed by Cölfen's group in 2008 as part of the OpenAUC project (Strauss et al. 2008; Cölfen et al. 2010), and later updated with a mirror based optical system, which significantly reduces chromatic aberration (Pearson et al. 2018). Software for the analysis of MW-AUC data was first presented in 2015 (Gorbet et al. 2015). In 2016, Beckman-Coulter released the Optima AUC™ series, which is equipped with Rayleigh interference and UV/visible

✉Borries Demeler demeler@gmail.com.

Supplementary Information The online version contains supplementary material available at https://doi.org/10.1007/s00249-023-01640-5.

multi-wavelength absorption optics. In contrast to the Cölfen optics, which uses a fiber and a CCD spectrophotometer to measure over 1000 wavelengths simultaneously, the Optima AUC records multiple wavelengths individually, and sequentially, using a monochromator stepping motor and a photomultiplier tube. The latter approach is much slower than the CCD approach, but offers significantly higher sensitivity in the low UV where most biopolymers absorb. A detailed discussion about the different hardware approaches and their pros and cons can be found in reference (Henrickson et al. 2022). MW-AUC shares the strength of traditional single wavelength analysis to separate solutes based on their hydrodynamic properties in a physiological environment, where important parameters such as ionic strength, pH, temperature, analyte concentrations, and other factors can be modulated, and titrations can be performed to study dynamic interactions. MW-AUC adds an important dimension to this by exploiting differences in absorbance spectra from different types of solutes present in the same mixture. One of the most important advantages of MW-AUC is its ability to deconvolute individual solutes based on their intrinsic extinction spectra when these spectra can be obtained from isolated solutes, for example, before mixing them in a titration experiment. Another advantage of MW-AUC is that the signal-to-noise ratio increases significantly because data collection is performed at multiple wavelengths, increasing data density. MW-AUC has been successfully applied to applications studying biopolymers (see (Ahmed et al. 2022), and references in Henrickson et al. (2022)) as well as in material science (Karabudak et al. 2016).

MW-AUC analysis for data from all currently available instruments is well supported in the open source UltraScan software package (Demeler and Gorbet 2016), which supports both the Cölfen detector and the Beckman Optima AUC. As discussed in Henrickson et al. (2022), MW-AUC can be applied in two modes. First, if intrinsic absorbance spectra for all spectrally distinct solutes present in a mixture are available for the measured wavelength range, the individual solutes can be spectrally deconvoluted, generating separate hydrodynamic contributions for each solute. Second, for cases where individual spectra for each solute are not available, a MW-AUC experiment can be analyzed hydrodynamically for each wavelength independently, and a sedimentation coefficient distribution can be derived that plots the amplitudes of each hydrodynamically distinct solute as a function of wavelength. In such a plot, the spectral pattern of each species will be apparent, and can aid in the interpretation of the experimental data.

For the first case, a linear combination of the absorbance spectra is fitted by non-negatively constrained least squares (NNLS) (Lawson and Hanson 1995) to the multi-wavelength data to obtain the amplitude of each spectrally unique species at each radial point, and at each time point of the experiment. So far, the UltraScan software is lacking a way to assess the quality of this fit and to ensure that the linear decomposition succeeds without introducing erroneous signal from a mismatch in the spectral basis functions. This could occur, for example, when hypo/hyperchromic shifts occur during complex formation, altering the original absorbance spectra. It is, therefore, important to monitor the quality of the decomposition fit. To address this limitation, a new module was added to the UltraScan decomposition program to allow the user to monitor the fitting residuals graphically and statistically. The program displays the residuals from the spectral deconvolution as

a function of wavelength and radial positions in a three-dimensional plot and provides functionality to inspect individual wavelength profiles for each radial position and scan time.

Methods

Basis spectra determination

Bovine thyroglobulin was purchased from Sigma-Aldrich (catalog number T1001). Double-stranded DNA was prepared by E. coli amplification of pPOL1–208–12 (Georgel et al. 1993) and subsequent purification of the plasmid DNA, followed by digestion with Eco RI restriction endonuclease (New England Biolabs) and purification of a 196 bp fragment by anion exchange and size exclusion chromatography. The protein and purified DNA fragment were dissolved in a buffer containing 10 mM tris (hydroxymethyl) aminomethane, 150 mM sodium chloride, and 20 mM calcium chloride. The concentration of both analytes was adjusted to 1.0 OD at 280 nm for thyroglobulin and 260 nm for DNA. Before mixing thyroglobulin and plasmid DNA, three serial dilutions (1:2) were prepared and the UV spectra of the stock solutions and the three dilutions were measured on a Genesys S10 spectrophotometer between 240 and 290 nm. The UltraScan spectrum fitter module was then used to globally fit all dilution spectra to a sum of Gaussian functions to derive an intrinsic extinction spectrum for plasmid DNA and Thyroglobulin. The extinction spectra were normalized for 1.0 OD at 260 nm for the DNA and 1.0 OD for thyroglobulin (see Fig. 1). The spectral profiles were then used for the multi-wavelength decomposition. To maintain absorbance within the optimal dynamic range of the UV detector across the entire measured wavelength range, the stock solutions for thyroglobulin and DNA were diluted to 0.6 OD at 260 nm for the DNA, and 0.6 OD at 280 nm for the protein, and mixed in a 1:1 ratio by volume for use in the analytical ultracentrifuge.

MW-AUC experiments

A MW-AUC experiment was performed at 20 °C using a Beckman-Coulter Optima AUC at the Canadian Center for Hydrodynamics at the University of Lethbridge. 0.46 ml of the DNA/thyroglobulin mixture was loaded into a 2-channel, 12 mm standard epon centerpiece and measured at 36,000 rpm for 10 h. Intensity data were collected at every second wavelength between 240 and 290 nm, resulting in 72 scans for each of the 26 wavelengths. Experimental data were fitted with the two-dimensional spectrum analysis (2DSA) (Brookes et al. 2010), removing time- and radially invariant noise, and fitting the boundary conditions. A sedimentation coefficient range between 1 and 40 ($\times 10^{-13}$ s) with 100 grid points and a frictional ratio range from 1 to 10 with 60 grid points was used in the 2DSA analysis. The solution was refined with an iterative 2DSA using 10 iterations, for each wavelength, resulting in final RMSD values of 0.00213 −/ + 0.00032 for all 26 wavelengths. In the next step, a time-synchronized MW-AUC dataset was simulated based on the iterative 2DSA models, aligning scans from all wavelengths to identical time points for each wavelength. The simulated data were deconvoluted by spectral decomposition using the spectral basis profiles determined earlier to obtain the contributions from each solute (thyroglobulin and DNA).

Multi-wavelength decomposition

MW-AUC is a method for hydrodynamically separating the absorbance profiles of interacting or non-interacting analytes when each analyte contributes a unique profile to the overall absorbance observed in the AUC experiment. However, this technique relies on some assumptions that should be verified. First, mixing of two or more absorbing solutes should not induce a change in the absorbance properties of each analyte, especially when these solutes interact. Second, the absorbance spectra of the analytes should be linearly independent of each other. To check this linearity, the angle between each pair of the analyte's molar extinction vectors $U(u_1, u_2, \ldots, u_n)$ and $V(v_1, v_2, \ldots, v_n)$ can be checked in the UltraScan spectral decomposition module according to Eq. 1 (Walter et al. 2015), where u_i and v_i are the corresponding extinction coefficients from analytes U and V, respectively, at each wavelength.

$$\theta = \arccos\left(\frac{U \cdot V}{\| U \| \cdot \| V \|}\right). \quad (1)$$

As the angle θ increases from zero to 90°, the linear dependency between the two extinction coefficient vectors decreases. In other words, when $\theta = 0°$, the spectra of the two analytes are identical and cannot be resolved, but at $\theta = 90°$, the extinction coefficient vectors are perfectly perpendicular (zero overlap) and linearly independent. An angle of 90 ° is an ideal situation that is unlikely being observed in an experiment. While in theory any set of spectra with an angle greater than zero can be separated, separation between the spectra improves as the angle θ approaches 90 °. For cases with significant spectral overlap (a small θ), expanding the measured wavelength range is often helpful. In our case, the angle between the spectra of thyroglobulin and DNA, measurements between 250 and 280 nm results in an angle of $\theta = 18.6°$, but increasing the wavelength range from 240 to 290 nm, increases orthogonality and $\theta = 25°$, offering a significantly improved resolution.

For the next step, the UltraScan module *us_mwl_species_fit* is used to decompose simulated data into the protein and DNA absorbance profiles. The program performs the linear decomposition of the wavelength scan, returning a non-negative scalar value for the amplitude of each spectral component contributing to the wavelength data for each radial position and time point of a scan. This process is illustrated in Eq. 2:

$$A(r,t) = \sum_{i=1}^{N} x_i \,.\, E_i(\varepsilon_{i,1}, \varepsilon_{i,2}, \ldots \varepsilon_{i,3}). \quad (2)$$

In the above equation, ***A(r, t)*** is the absorbance vector for M wavelengths at radial position r and scan time t. x_i is a non-negative scalar value indicating the relative contribution of solute i to the wavelength scan with extinction spectrum E_i and extinction coefficients $\varepsilon_{i,j}$. This fit employs the non-negatively constrained least squares fitting algorithm NNLS (Lawson and Hanson 1995). By repeating the same procedure for all radial points and scan times, the two-dimensional sedimentation profiles for each spectral basis component are reconstructed.

NNLS fit quality monitoring

NNLS (Lawson and Hanson 1995) is used to solve the matrix inversion problem (Eq. 2) and find the unknown parameters of x_i. By obtaining these coefficients and reusing Eq. 2, absorption profiles at different wavelengths are reconstructed for the fitted data. The difference between the decomposed and simulated profiles produces an array of residuals (fitting errors) for each wavelength. This array has two features helpful in assessing the quality of the decomposition. The first is the amplitude of the fitting errors, which is conveniently represented by the average error. This value can be compared to the signal-to-noise ratio and should not exceed the root mean squared deviation (RMSD) obtained in the hydrodynamic data modeling step. Second, the array can be used to test the randomness of the decomposition residuals. Any non-random errors indicate that the component's extinction profiles used in the decomposition process are insufficient to properly deconvolute the spectral contributors to the absorbance spectra. Such a situation can occur when mixing of individual components in the solution induces a change in the spectral properties of one or more solutes in the mixture, and, for example, experiences a hyper- or hypochromic shift in its absorbance profile when forming a complex. Other possibilities for deviation include non-linearity in the recorded absorbance data, which can occur if the dynamic range of the detector is exceeded. If the distribution of residuals is not random, the decomposition should be further investigated to correct the cause for the non-randomness of the residuals. Several statistical methods are available to check whether the vector of residuals is randomly distributed. A suitable test is the Wald–Wolfowitz runs test, which is a non-parametric statistical test for a two-valued data sequence (Zar 2010). The run is defined as a series of binary values, which in our case is given by the sign of the residual error e_{ij} at each radial point i at time j when comparing the experimental absorbance, a_{ij}, with the corresponding fitted value, d_{ij} (see Eq. 3).

$$e_{ij} = a_{ij} - d_{ij}\,. \tag{3}$$

Residuals above the median (fitted) value are coded positive and values below the median are considered negative values. After converting to a binary array of positive and negative values, the number of runs is calculated by counting the occurrences of the positive-to-negative or negative-to-positive jumps ("runs") along the sequence. The runs test assumes that each value in the array is independently drawn from a random distribution. To check the hypothesis, the mean (μ) and standard deviation (σ^2) of the array can be calculated, and then compared to the mean and standard deviation of a truly random distribution by way of the Z value, given by Eq. 4:

$$\mu = \frac{2N_1N_2}{N_1+N_2} + 1, \sigma^2 = \frac{2N_1N_2(2N_1N_2 - N_1 - N_2)}{(N_1+N_2)^2(N_1+N_2-1)}, Z = \left|\frac{N_{runs} - \mu}{\sigma}\right|. \tag{4}$$

where N_1, N_2, N_{runs}, and Z are the number of negative values, number of positive values, number of runs, and the runs statistic test, respectively. The runs test rejects the null hypothesis if $Z > 1.96$, and a value of Z above 1.96 indicates that the sequence is non-random. Using this method, each wavelength decomposition can be checked to ascertain that the fit generates a randomly distributed decomposition error. The approach described above

is called the normal approximation approach, assuming that the number of the negative and positive values (one for each wavelength) are greater than 20. For samples smaller than 20, a criterion for randomness can be obtained from published tables (Kanji 2006), which have been programmed in UltraScan. A second metric for the randomness of the residuals is the p-value. It indicates how similar the residual sequence is to a truly random sequence. A value of 1.0 indicates a perfectly random sequence, decreasing values indicate that the fit has increasing amounts of systematic error.

Results

Figure 2 shows an example decomposition of the MMAUC sedimentation velocity experiment of the thyroglobulin/DNA mixture. In the time-synchronized multi-wavelength data set shown in Fig. 2A, two well-separated boundaries are apparent. The slower boundary reflects the DNA fragment, while the faster sedimenting boundary reflects thyroglobulin, and aggregates thereof. These patterns are faithfully reproduced as separated experiments (DNA in Fig. 2B, thyroglobulin in Fig. 2C). Furthermore, it is clear to see that the sum of the absorbances of the data shown in Fig. 2B and C equal the absorbance of the scans shown in Fig. 2A. Integral sedimentation coefficient distributions from a two-dimensional spectrum analysis of the spectrally separated thyroglobulin and DNA data are shown in Fig. 3. The analysis shows that the DNA fragment is homogeneous and sediments at ~ 6.0 s, while thyroglobulin is very heterogeneous, containing varying aggregation states between 10 and 40 s. From these results, it can be concluded that the DNA fragment does not bind to thyroglobulin, since there is no sedimentation coefficient overlap between the two species. Also, the relative amounts of the different aggregation states of thyroglobulin can be clearly distinguished (~ 15% between 10 and 20 s, ~ 60% at 20 s, ~ 25% above 20 s).

Program controls

The graphical user interface (GUI) for the spectral decomposition residual visualization module is invoked from the spectral decomposition module (SI 1), and offers multiple controls that permit the user to customize the display, inspect residual patterns and review statistics (Fig. 4). The residual patterns are functions of wavelength, radius and time, which requires a four-dimensional visualization approach. The GUI offers two tabs. The first tab shows a three-dimensional (3D) surface plot of the residual errors from the decomposition as a function of radius and wavelengths for a user selected scan (Fig. 4, upper panel). The inspected scan can be selected from a drop-down box or sequentially with a bi-directional button to traverse the fourth dimension. All statistics and plots are updated automatically as the user scrolls through the available scans. The user has the option to either display the absolute magnitude of the residual, or the actual residual value, which can be negative. This options allows the user to check which part of the radial and wavelength dimensions contributes the largest error to the fitting process.

A list provides the RMSD of the entire 4D decomposition, as well as the largest negative and positive residual value for reference. The wavelength and radius range to be displayed can be modified by setting minimum and maximum range limits. Additional display options include the possibility to select a theme, a preset or custom camera angle, and a color

map. An export function allows the user to render all, or a sub-selection, of scans to a series of screen captures for subsequent assembly into a 3D movie. Movies of the residual patterns for the DNA and thyroglobulin decomposition for the entire MW-AUC experiment are shown in Supplemental Information SI 2, rendered as real residuals, and in SI 3 showing the absolute magnitude of the residuals. The rendering quality of the image can be user-defined. Additional controls allow the user to select a radius or wavelength slice from the four-dimensional dataset (to be displayed in a two-dimensional format), or to select any point in the 3D surface to obtain the corresponding residual values.

In the second tab, the wavelength decomposition for an individual radial position for a single scan can be inspected. 2D graphs of the simulated data and fitted data, as well as the error values over the wavelengths are plotted (Fig. 4, lower panel). After decomposition, the user selects a single scan from all available scans, and using a slider widget, can traverse the wavelength decompositions for all radial positions between meniscus and cell bottom for the selected scan. A panel below the 2D plots automatically provides detailed statistics for the radial position in the current view. The following statistics are provided: 1. The average magnitude and median of the residuals, and the number of residuals shown; 2. The number of negative and positive residuals, and the number of runs; 3. For each runs test, the program displays the test value, the p-value and the critical value, above which the decomposition is classified as non-random.

A display field indicates in green if the residual pattern is considered to be random, or in red, if it is considered to be non-random. Finally, a pixel map can be displayed to visualize the randomness state of all radial points versus all scans (see Fig. 5). The pixel map indicates a significant proportion of non-random decomposition results, with the majority of the non-random pixels resulting from decompositions in the region closer to the bottom of the cell. Since thyroglobulin is clearly sedimenting much faster than the DNA, representing the majority of the signal closer to the bottom of the cell, it can be concluded that the non-randomness results primarily from the thyroglobulin spectral contribution. A possible explanation would be a shift in the absorbance pattern of aggregated thyroglobulin, perhaps caused by Mie scattering from larger aggregates, which was not captured in the non-aggregated thyroglobulin spectra collected earlier in the dilution series. Such diagnostics inform the troubleshooting process essential for the analysis of MW-AUC experiments.

Summary

Residual patterns are a critical aspect of the result quality derived from fitting experimental data to simulated models. Stochastic noise in experimental data is unavoidable and is the reason why models fitted to experimental data never produce a unique solution. There are infinitely many solutions that produce the same RMSD for a given dataset containing stochastic noise. The resulting model has the best chance to be a valid representation of the underlying system only if random residuals are observed. Systematic deviations in the residual pattern point to problems with the model, and require adjustment of the model to account for missing contributions, or demand more robust fitting algorithms that avoid local minima. Alternatively, when adjustments of the model are not possible, the hypothesis of the model must be rejected.

A new UltraScan module described here allows the user to investigate the residual error patterns for a NNLS decomposition for any radial position and scan from a MW-AUC experiment, and represents the error by 3D data visualization, and quantifies it by inspecting statistical metrics like RMSD and the runs test. The program can process MW-AUC data from both a multi-scan velocity experiment, or a single scan sedimentation equilibrium profile. Complex, multi-dimensional data such as multi-wavelength sedimentation velocity experiments are challenging to evaluate, the module presented here provides a mechanism to evaluate spectral decomposition results from MW-AUC analyses using an intuitive interface to obtain a rigorous statistical and visual error analysis which will improve MW-AUC interpretation as well identification of error sources, and could prove useful as a model for other multi-dimensional experimental validation.

Supplementary Material

Refer to Web version on PubMed Central for supplementary material.

Acknowledgements

This research and S.M. were supported by the Biomolecular Interaction Technology Center, University of Delaware, and the Canada 150 Research Chairs program (C150-2017-00015), the Canada Foundation for Innovation (CFI-37589), the National Institutes of Health (1R01GM120600) and the Canadian Natural Science and Engineering Research Council (DG-RGPIN-2019-05637) – all grants to BD.

Data availability

All data are stored in openAUC format (see: Cölfen et al. 2010) on the LIMS server for the Canadian Center for Hydrodynamics at the University of Lethbridge and are available upon request from the author.

References

Ahmed I, Hahn J, Henrickson A, Khaja FT, Demeler B, Dubnau D, Neiditch MB (2022) Structure-function studies reveal ComEA contains an oligomerization domain essential for transformation in gram-positive bacteria. Nat Commun 13(1):7724 [PubMed: 36513643]

Brookes E, Cao W, Demeler B (2010) A two-dimensional spectrum analysis for sedimentation velocity experiments of mixtures with heterogeneity in molecular weight and shape. Eur Biophys J 39(3):405–414 [PubMed: 19247646]

Cölfen H, Laue TM, Wohlleben W, Schilling K, Karabudak E, Lang-horst BW, Brookes E, Dubbs B, Zollars D, Rocco M, Demeler B (2010) The open AUC project. Eur Biophys J 39(3):347–359 [PubMed: 19296095]

Demeler B (2019) Measuring molecular interactions in solution using multi-wavelength analytical ultracentrifugation: combining spectral analysis with hydrodynamics. The Biochemist. Chapter 3. Editor: Willmott Chris, Portland Press, pp. 14–18.

Demeler B, Gorbet G (2016) Analytical ultracentrifugation data analysis with UltraScan-III Chapter 8. In: Uchiyama S, Stafford WF, Laue T (eds) Analytical Ultracentrifugation: Instrumentation, Software, and Applications. Springer, pp 119–143

Georgel P, Demeler B, Terpening C, Paule MR, van Holde KE (1993) Binding of the RNA polymerase I transcription complex to its promoter can modify positioning of downstream nucleosomes assembled in vitro. J Biol Chem 268:1947–1954 [PubMed: 8420969]

Gorbet GE, Pearson JZ, Demeler AK, Cölfen H, Demeler B (2015) Next-generation AUC: analysis of multiwavelength analytical ultracentrifugation data. Methods Enzymol 562:27–47 [PubMed: 26412646]

Henrickson A, Gorbet GE, Savelyev A, Kim M, Hargreaves J, Schultz SK, Kothe U, Demeler B (2022) Multi-wavelength analytical ultracentrifugation of biopolymer mixtures and interactions. Anal Biochem 1(652):114728

Kanji GK (2006) 100 statistical tests, 3rd edn. Sage Publications Ltd

Karabudak E, Brookes E, Lesnyak V, Gaponik N, Eychmüller A, Walter J, Segets D, Peukert W, Wohlleben W, Demeler B, Cölfen H (2016) Simultaneous identification of spectral properties and sizes of multiple particles in solution with Subnanometer resolution. Angew Chem Int Ed Engl 55(39):11770–11774 [PubMed: 27461742]

Lawson CL, Hanson RJ (1995) Solving least squares problems. Soc Ind Appl Math. 10.1137/1.9781611971217

Pearson J, Walter J, Peukert W, Cölfen H (2018) Advanced multiwave-length detection in analytical ultracentrifugation. Anal Chem 90(2):1280–1291 [PubMed: 29214799]

Strauss HM, Karabudak E, Bhattacharyya S, Kretzschmar A, Wohlleben W, Cölfen H (2008) Performance of a fast fiber based UV/Vis multiwavelength detector for the analytical ultracentrifuge. Colloid Polym Sci 286(2):121–128 [PubMed: 19816525]

Walter J, Sherwood PJ, Lin W, Segets D, Stafford WF, Peukert W (2015) Simultaneous analysis of hydrodynamic and optical properties using analytical ultracentrifugation equipped with multi-wavelength detection. Anal Chem 87(6):3396–3403 [PubMed: 25679871]

Zar JH (2010) Biostatistical analysis, 5th edn. Prentice Hall/Pearson

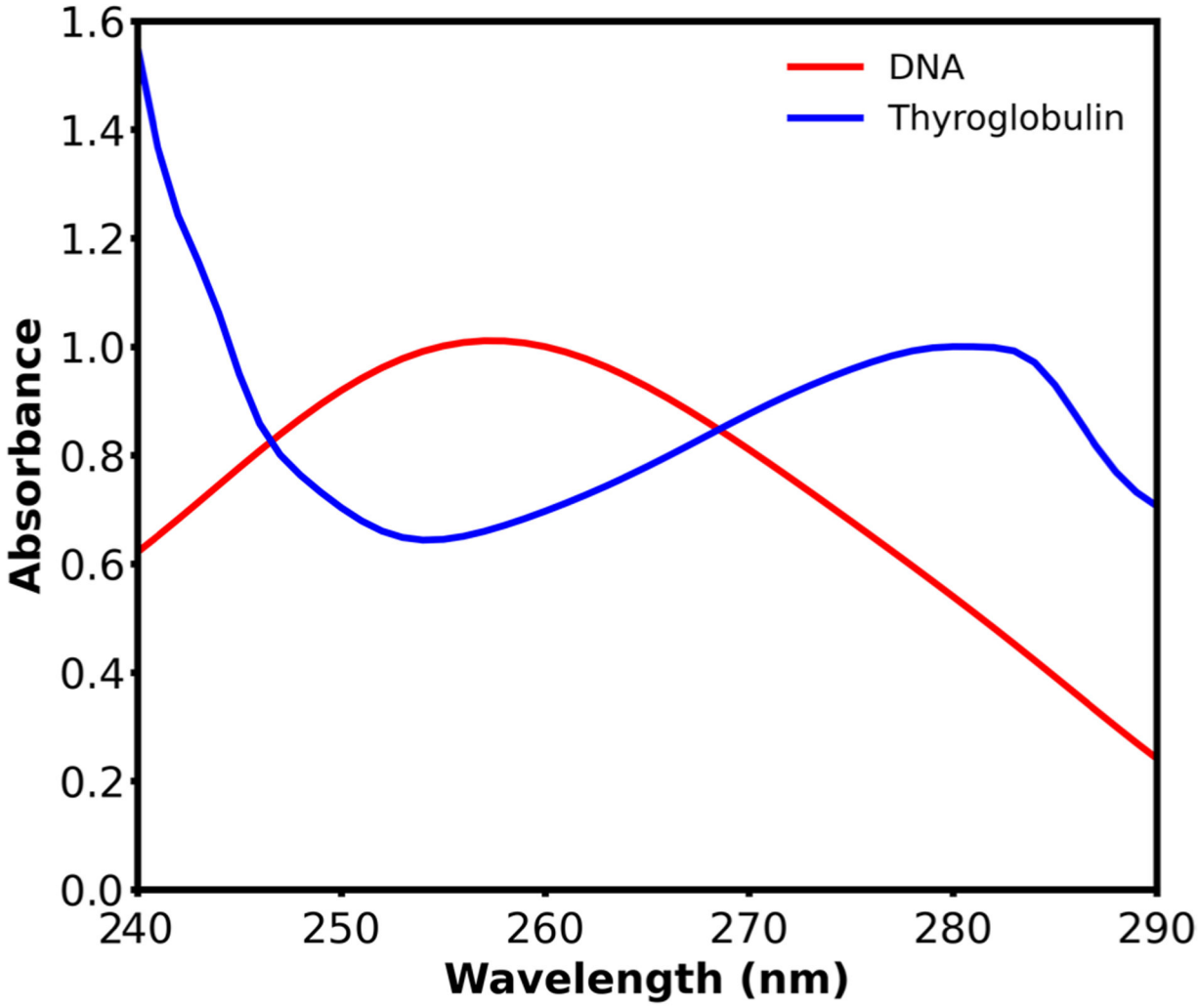

Fig. 1.
Extinction spectra of thyroglobulin and DNA fragment between 240–290 nm

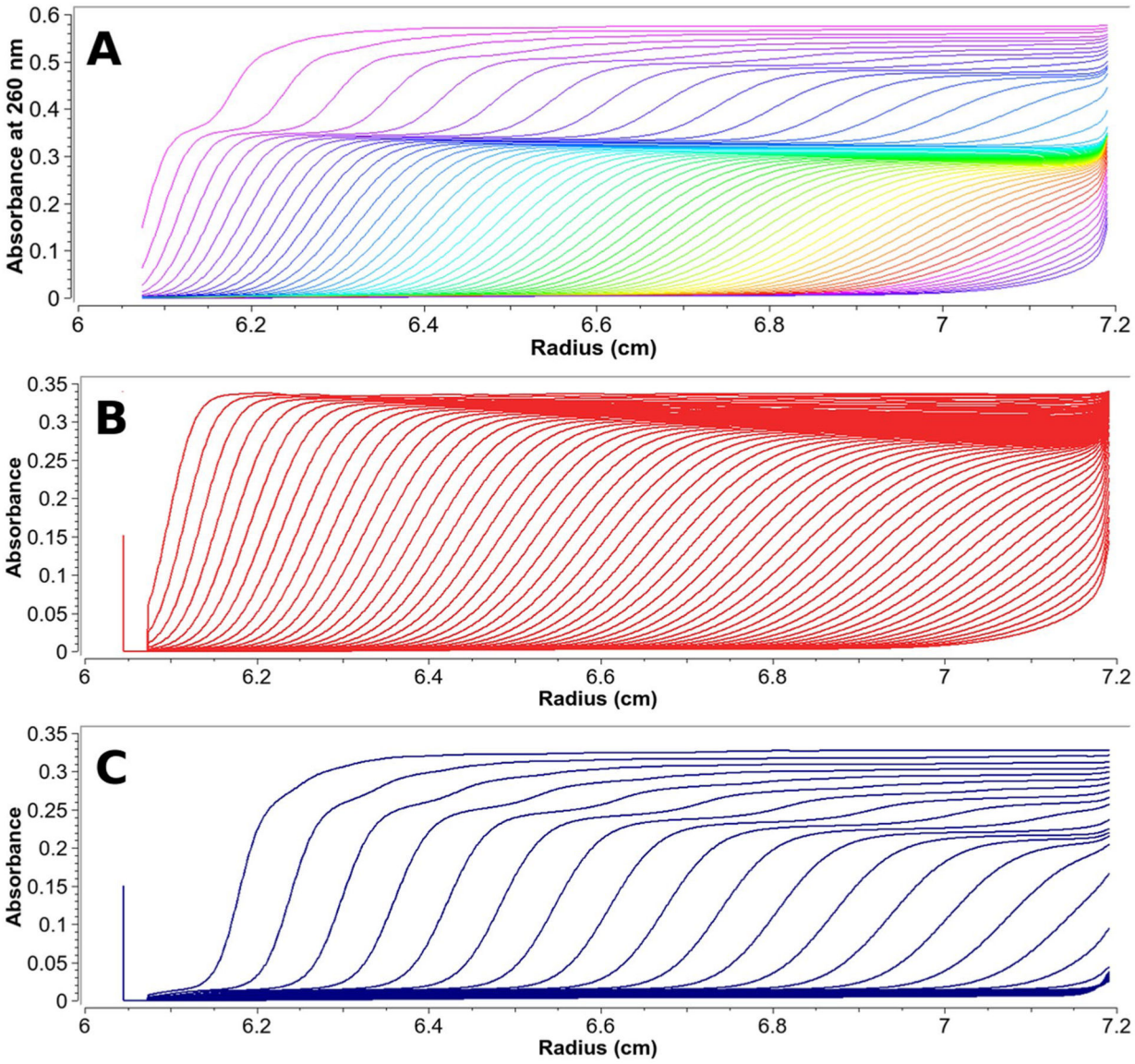

Fig. 2.

A Absorbance profile of the time-synchronized data at 260 nm. Multi-wavelength decomposed profiles of the **B** plasmid DNA (red) and **C** thyroglobulin (blue)

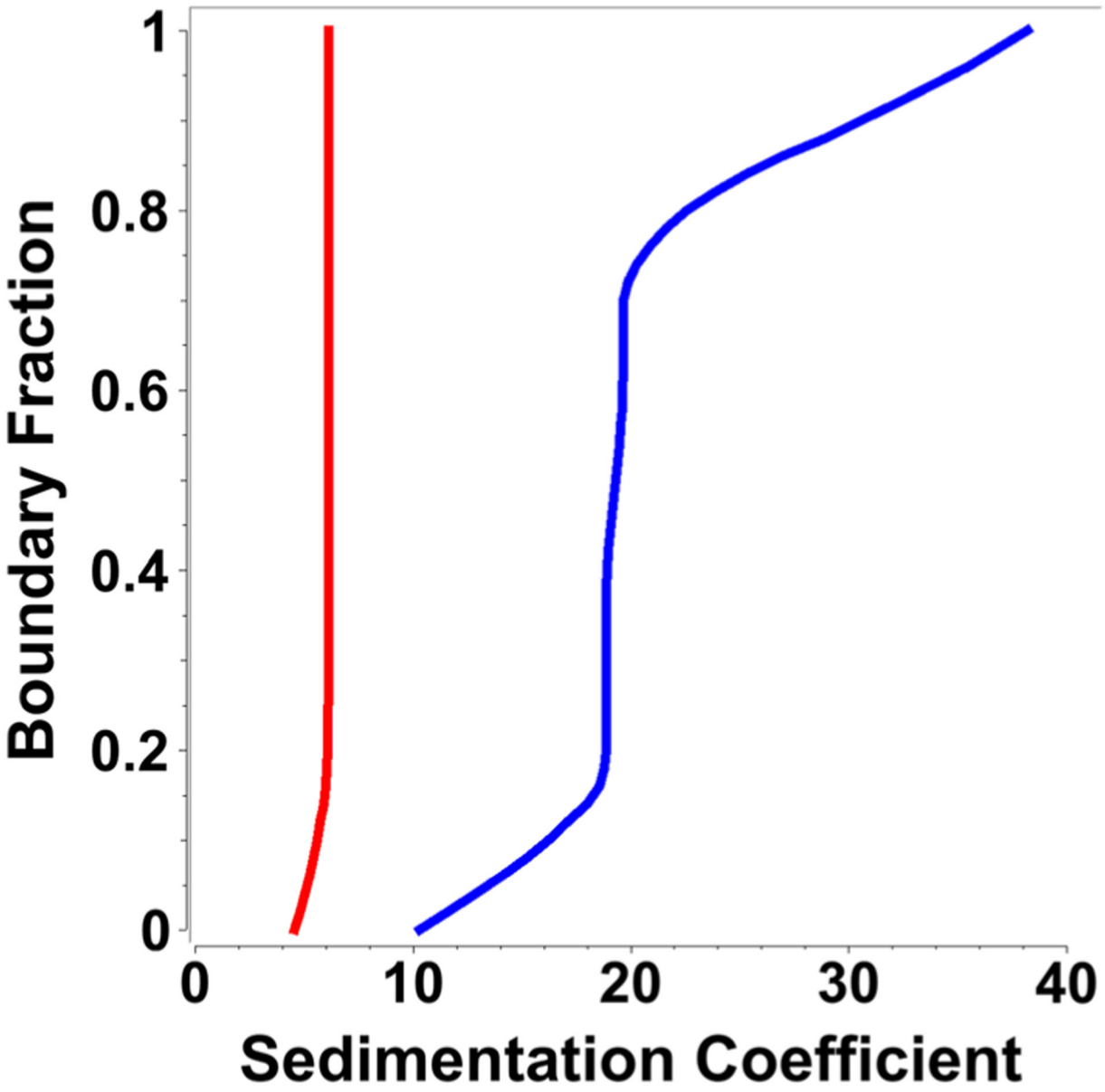

Fig. 3.

Integral sedimentation coefficient distribution from a two-dimensional spectrum analysis performed on the spectrally separated homogeneous DNA fragment (red, ~ 6.0 s) and the aggregated thyroglobulin protein (blue, ~ 10–40 s)

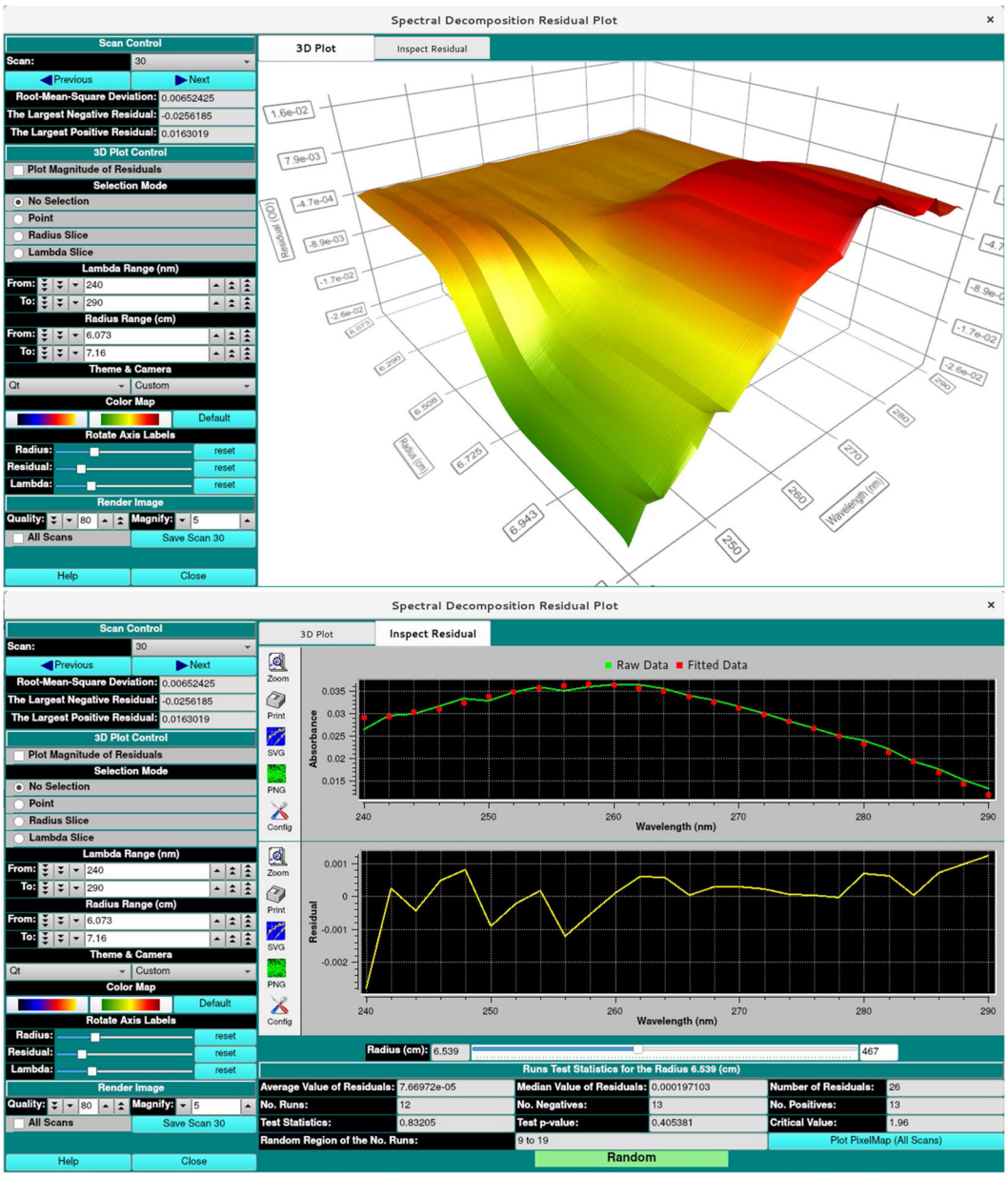

Fig. 4.

Screenshot of the spectral decomposition residual visualization module. The upper panel shows the 3D visualization tab, the lower panel shows the controls for the statistical analysis of the decomposition

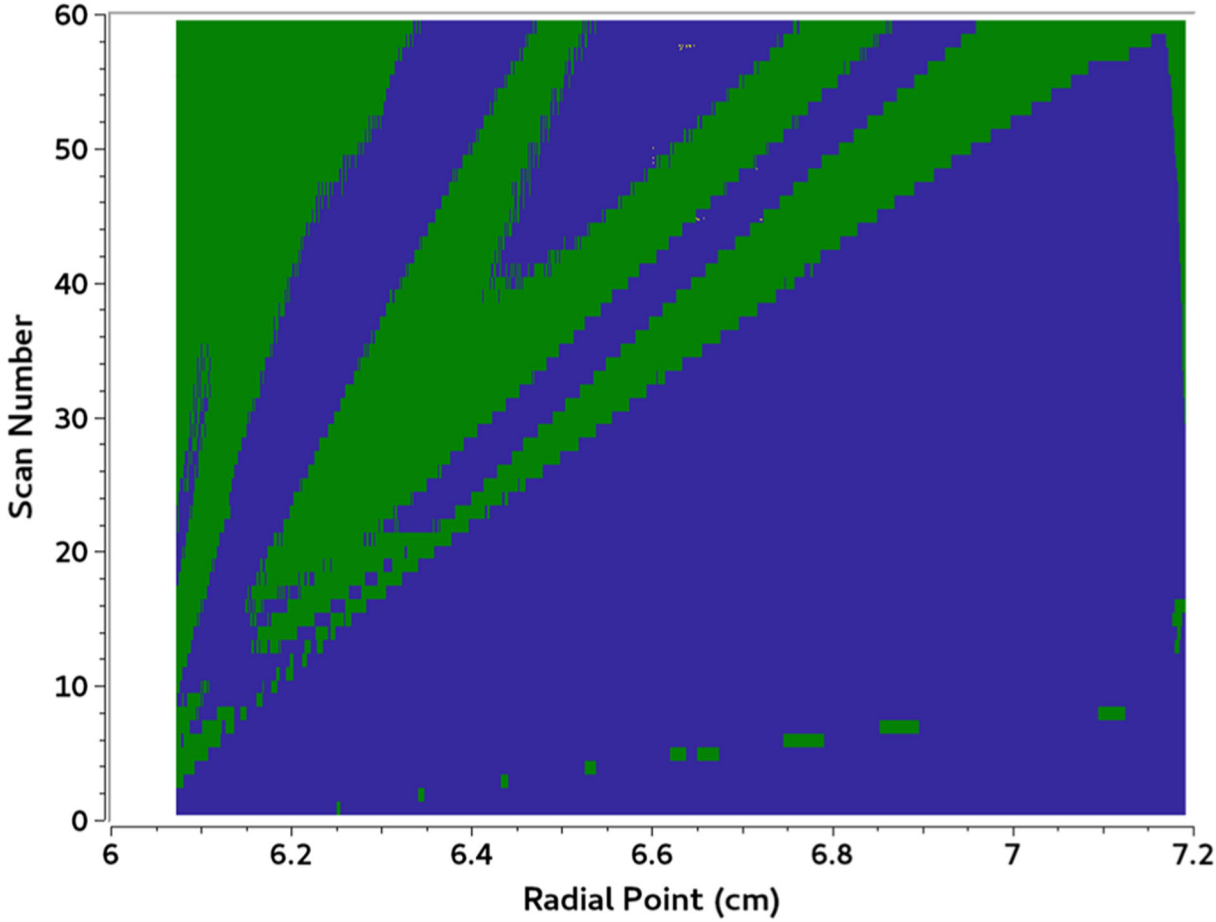

Fig. 5.

2D contour of radial positions' randomness state. Blue and green pixels are used to show the non-random and random fitting error, respectively, for each scan as a function of radius